Published in final edited form as:
Phys Rev Lett. 2005 January 21; 94(2): 028103.

Control of Traveling Waves in the Mammalian Cortex

Kristen A. Richardson[1,2], **Steven J. Schiff**[1,3,4], and **Bruce J. Gluckman**[1,2,3,*]

1 *Krasnow Institute for Advanced Study, George Mason University, Fairfax, Virginia 22030, USA*

2 *Department of Physics and Astronomy, George Mason University, Fairfax, Virginia 22030, USA*

3 *Program in Neuroscience, George Mason University, Fairfax, Virginia 22030, USA*

4 *Department of Psychology, George Mason University, Fairfax, Virginia 22030, USA*

Abstract

We experimentally confirmed predictions that modulation of the neuronal threshold with electrical fields can speed up, slow down, and even block traveling waves in neocortical slices. The predictions are based on a Wilson-Cowan–type integro-differential equation model of propagating neocortical activity. Wave propagation could be modified quickly and reversibly within targeted regions of the network. To the best of our knowledge, this is the first example of direct modulation of the threshold to control wave propagation in a neural system.

Traveling waves in excitable media are commonly observed in physical [1,2], chemical [3], and biological [4–6] systems. Mathematical models have been developed in conjunction with these experimental systems to provide a deeper understanding of the dynamics and infer how individual experimental parameters of the system, such as threshold, contribute to these dynamics [5,7–10]. Rapid access to system parameters would offer the means to control pattern formation and dynamics in these systems.

Successful modulation of dynamics has been accomplished in chemical, cardiac, and neural systems. In the Belousov-Zhabotinsky chemical reaction system, modulation of excitability through local changes in illumination of a light sensitive catalyst allowed control of wave propagation [11]. Electric fields modulated activity propagation in heart tissue [12]. The propagation speed of excitation waves in neocortex has been slowed by pharmacologically interfering with chemical synaptic transmission [13].

It has been previously shown that electric fields can modulate neuronal thresholds by quickly and reversibly polarizing asymmetric neurons [14]. Electric fields as small as 140 μV/mm have been observed to modulate neural firing [15]. Polarization occurs on time scales of about 20 ms and can be maintained for many seconds or minutes [16]. Applied electric fields have been used to adaptively control seizure formation *in vitro* [17], modulate epileptiform activity *in vivo*, and dynamically probe activity changes associated with impending seizures [18].

We show here that electric fields can quickly alter traveling wave dynamics in ways predicted by theory through direct modulation of neuronal threshold. To our knowledge, this is the first report of control of wave propagation through direct modulation of excitability threshold in any neural system.

Wilson and Cowan [19] developed a set of integro-differential equations to form a continuum model of cortex which demonstrated traveling waves. This model was recently modified [20] to represent traveling pulse propagation in disinhibited neocortex [21]. The model predicts that

*Electronic address: bgluckma@gmu.edu.

threshold determines several dynamical properties of the traveling wave as shown in the next few paragraphs. Specifically, at low threshold waves travel faster than at high threshold.

The model is

$$\frac{\partial u(x,\ t)}{\partial t} + u(x,\ t) = \int_{-\infty}^{\infty} w(x - x')P(u(x',\ t) - \theta)dx' - v(x,\ t),$$
$$\frac{1}{\epsilon}\frac{\partial v(x,\ t)}{\partial t} + \beta v(x,\ t) = u(x,\ t). \quad (1)$$

The variable u represents neural activity, the fractional firing rate of the local neurons. Activity at position x at time t, $u(x; t)$, is a function of the activity of the whole population with spatial connectivity w. Activation at position x depends on $u(x'; t)$ with respect to a threshold value θ through the function P. As in [20], we choose P to be the Heaviside step function such that synaptic input comes only from positions with activity above threshold. A recovery variable, $v(x; t)$, accounts for activity accommodation and adaptation which contribute to refractoriness in the wake of activity. The parameter ∈ is the relative time constant for changes in recovery (v) versus activity (u) and is typically small. We set the parameter β to 0, though results are similar for β small.

We assume a traveling wave solution, $u(x; t) = U(x - ct) = U(z)$. Boundary conditions for a single, left-going traveling pulse are chosen such that U goes to zero at infinity, and is equal to threshold θ at 0 and a (see Fig. 1, inset), that is, $U(0; a) = \theta$, $U(\pm\infty) = 0$. Equation (1) then collapses to a linear second order differential equation $-c^2U'' + cU' - \epsilon U = c(w(z) - w(z) - a))$. With w chosen to be $w(z) = e^{-|z|}/2$, the analytical solution is partitioned into three regions: (1) $z < 0$, (2) $0 < z < a$, and (3) $a < z$, and can be written as $U(z) = A_i e^{z} + B_i e^{-z} + C_i e^{\lambda_+ z} + D_i e^{\lambda_- z}$. Here i denotes the solution region [(1), (2), or (3)] and the exponent $\lambda_\pm$ is determined from the homogeneous solution to the differential equation. We match the four coefficients at the boundaries, $U(0)$ and $U(a)$, to numerically determine the relationships between the four parameters of the system: relative time constant (∈), pulse speed (c), pulse width (a), and threshold (θ). Pulse speed and width are shown in Fig. 1 as a function of threshold for several values of ∈ (solid and dashed lines).

There exist either two or no solutions for speed and width for a given pair of threshold and relative time constant values. When there are two solutions (at smaller θ), the smaller width and speed solution (Fig. 1, gray region) is thought to be unstable [20]. A similar situation was noted by Amari for a field model of stationary pulses of activity in a network of neurons [22] and found by Rinzel *et al.* for analogous problems in a model of traveling pulses in axons [6]. The unstable solutions in the gray region (Fig. 1) are unlikely to be observed experimentally. At very small θ, we cannot calculate the stable branch of the solutions due to numerical instability. At large values of threshold, both solutions disappear, and all pulses decay. Note that the solutions disappear at finite values of width and speed, analogous to the ‘‘velocity gap’’ prediction for crack propagation [23].

Thus, these equations predict for the stable solution that speed and width depend on threshold such that at low threshold the pulses are wide and fast (large a and c, respectively), and at higher threshold the pulses are narrow and slow (small a and c). As threshold is increased, propagation will fail at nonzero speed and width.

We therefore predicted that we could speed up, slow down, and block propagating neural activity in neocortical slices with the application of electric fields. Furthermore, we predicted that we could affect wave propagation either globally, over the whole slice, or locally, in a specific region of the slice, by changing the geometry of the applied field.

Transverse neocortical slices (400 μm thick) prepared from adult male Sprague-Dawley rats (age 26–68 days) were bathed in 32° artificial cerebrospinal fluid (130 NaCl, 1.25 NaH_2PO_4, 3.5 KCl, 23.9 $NaHCO_3$, 1.1 $MgSO_4$, 10 dextrose, 1.23 $CaCl_2$, in mM) containing low doses (4.7–8.3 μM) of picrotoxin, a blocker of γ-aminobutyric acid-A ($GABA_A$) inhibitory transmitter. Previous work on propagation of activity in neocortical slices bathed in low doses of picrotoxin revealed that layer 5 neurons are necessary for supporting the initiation and the transmission of activity [24]. These layer 5 neurons have long apical dendrites and are easily polarizable with electric fields applied parallel to the dendrite-soma axis. Therefore, this system is amenable to electric field modulation for altering propagation.

A bipolar stimulation electrode (Fig. 2, SE) was placed in layers 5–6 at one end of the slice to initiate epileptiform bursts that propagated parallel to the pial surface [25,26]. An electric field was applied across the entire slice [global field, Fig. 2(a)] or across a localized region of the slice [local field, Fig. 2(b)] using custom built voltage or current controlled circuitry and nonpolarizing (Ag/AgCl) electrodes [Figs. 2(a) and 2(b): FE1, FE2]. We define a positive electric field as one oriented from apical dendrites to soma [Fig. 2(c)]. Such a field decreases the somatic transmembrane voltage difference from rest, brings the neuron closer to firing threshold, and is therefore excitatory.

Wave propagation was initiated with a short current pulse (0.15 ms, 0.1–1.0 mA) applied through an *RC* circuit to the bipolar stimulation electrode. The amplitude of the pulse was fixed for the duration of the experiment at a level determined to reliably initiate propagating activity. A waveform generator (Hewlett-Packard 33120A) was used to program a multiphasic periodic electric field (100–125 mHz), consisting of four phases: (1) positive, (2) zero, (3) negative, and (4) zero amplitude dc fields. Each phase corresponded to the application of a constant field for a duration of 2–2.5 s. Transitions between the phases were smoothed with a low frequency half sinusoid. To examine neuronal propagation speed as a function of applied field, waves were initiated by stimulating during the various phases of the waveform. Propagation speed was determined with at least 14 repetitions at each field amplitude for each phase.

Double barrel glass micropipette electrodes filled with 0.9% NaCl were used to differentially record local extracellular field activity in layers 2–3 with custom built pre-amplifiers (gain = 10) and an amplifier bank (DAGAN) with bandpass filter settings (1 Hz–1 kHz) and a gain of 200. The voltage recorded is associated with neuronal population electrical activity and is qualitatively related to the model parameter *u*. In the global field experiment, activity was recorded in two places in layers 2–3: near the wave initiation site and more distant from the initiation site (2–10 mm interelectrode distance). In the local field experiment, three recording electrodes were placed to record the propagating activity across the surface of the slice with the local field placed between either the first or the second pair of electrodes. Propagation speed was determined by the transit time between electrode pairs. In order to account for experimental drift, baseline speed as a function of time was determined with a polynomial regression fit during the zero field phases. Speed as a function of field is presented as a percentage of this baseline speed.

We observed modulation of propagation speed with globally applied electric fields in 25 of 25 slices. Examples of raw data are shown in Fig. 3(a). The black traces were recorded at R1 near the initiation site and the gray traces were recorded 2 mm along the propagation path at R2. The speed between R1 and R2 is field dependent: faster during the positive field (top traces) and slower during the negative field (bottom traces) relative to the zero field (middle traces). The speed normalized by the baseline speed is shown as a function of field amplitude for three typical experiments in Fig. 3(b) (larger graphs).

Sufficiently large negative fields (range 5–125 mV/mm, average 39 mV/mm) caused propagation failure in 18 of 25 slices. The rate of failure depended on the amplitude of the suppressive field [Fig. 3(b), smaller graphs]. Failure was defined when waves passed R1 but did not reach R2.

In some experiments, a high positive field (range 50–113 mV/mm, average 77 mV/mm) caused wave initiation prior to stimulation in eight of 25 slices. This caused apparent propagation failure of the stimulated waves due to refractoriness. This premature wave initiation at high positive fields could also be followed by aberrantly slow stimulated waves, as in the second experiment of Fig. 3(b), and occasional initiation failure (waves do not reach R1), as in the third experiment of Fig. 3(b) (open region in failure rate, experiment 3).

We observed modulation of propagation speed in 18 of 20 slices with locally applied electric fields. In these experiments, modulation was observed only in the region spanning the local field. In the other two of 20 slices, no clear speed modulation was observed. Examples of raw data are shown in Fig. 4(a). The field, which falls off radially, was larger and aligned with the dendrite-soma axis of neurons in the region spanned by R1 and R2 [see Fig. 2(b)], and smaller and not aligned with the neurons between R2 and R3. The time to travel between R2 and R3 was the same for all phases of applied field independent of field polarity. However, the time to travel between electrodes that spanned the field (R1–R2) was shorter during the application of positive field (upper traces) and longer during the application of negative field (lower traces), relative to zero field (middle traces).

The speed of propagation as a function of field is shown in Figs. 4(b) and 4(c) for two local field applications in different slices. In Fig. 4(b), the field was applied near the initiation site. The normalized speed is presented when the wave is near the field (R1–R2) and when the wave is far from the field (R2–R3). As with the global field, the speed of propagation increased between R1 and R2 as the field amplitude became more positive and decreased as the field amplitude became more negative. Alternatively, there was no change in speed with field amplitude in the region outside the local field (R2–R3). Similar results were seen when the field was applied farther from the initiation site [Fig. 4(c)] with speed modulation observed only across the field region (here, R2–R3).

It is important to note that electric field modulation occurs quickly. In these experiments stimulation for wave initiation was applied 700 ms after the transition between values of the electric field. Therefore, the modulation of the network behavior occurred on subsecond time scales.

We experimentally confirmed theoretical predictions that threshold modulation can increase or decrease the propagation speed of, and even block, cortical traveling waves. To the best of our knowledge, this is the first example of direct modulation of threshold to control wave propagation in a neural system. Such modulation could be applied rapidly in a locally precise manner. Since neural systems permit direct access to threshold, these findings open avenues to novel neural prosthetic applications including control and containment of seizure propagation.

References

1. T. E. Faber, Fluid Dynamics for Physicists (Cambridge University Press, Cambridge, 1995).
2. Schulman LS, Seidan PE. Science 1986;233:425. [PubMed: 17794566]
3. Zaikin A, Zhabotinsky AM. Nature (London) 1970;225:535. [PubMed: 16056595]
4. Carey AB, Giles RH Jr, McLean RG. Am J Trop Med Hyg 1978;27:573. [PubMed: 677370]
5. A. T. Winfree, The Geometry of Biological Time (Springer-Verlag, New York, 2001), 2nd ed.

6. Rinzel J, Keller JB. Biophys J 1973;13:1313. [PubMed: 4761578]
7. Cross MC, Hohenberg PC. Rev Mod Phys 1993;65:851.
8. Tyson JJ, Keener JP. Physica (Amsterdam) 1993;32D:327.
9. Rinzel J, Terman D, Wang XJ, Ermentrout B. Science 1998;279:1351. [PubMed: 9478895]
10. Bressloff PC. J Math Biol 2000;40:169. [PubMed: 10743600]
11. Sakurai T, Mihaliuk E, Chirila F, Sholwalter K. Science 2002;296:2009. [PubMed: 11988535]
12. Gray RA, Mornev OA, Jalife J, Aslanidi OV, Pertsov AM. Phys Rev Lett 2001;87:168104. [PubMed: 11690250]
13. Golomb D, Amitai Y. J Neurophysiol 1997;78:1199. [PubMed: 9310412]
14. Chan CY, Hounsgaard J, Nicholson C. J Physiol 1988;402:751. [PubMed: 3236254]
15. Francis JT, Gluckman BJ, Schiff SJ. J Neurosci 2003;23:7255. [PubMed: 12917358]
16. Bikson M, Inoue M, Akiyama H, Deans JK, Fox JE, Miyakawa H, Jefferys JGR. J Physiol 2004;557:175. [PubMed: 14978199]
17. Gluckman BJ, Nguyen H, Weinstein SL, Schiff SJ. J Neurosci 2001;21:590. [PubMed: 11160438]
18. Richardson KA, Gluckman BJ, Weinstein SL, Glosch CE, Moon JB, Gwinn RP, Gale K, Schiff SJ. Epilepsia 2003;44:768. [PubMed: 12790889]
19. Wilson HR, Cowan JD. Kybernetik 1973;13:55. [PubMed: 4767470]
20. Pinto DJ, Ermentrout B. SIAM J Appl Math 2001;62:206.
21. Neocortex contains a network of both excitatory and inhibitory neurons. Drugs can be applied to compromise network subpopulations, such as the inhibitory neurons, to alter the dynamics of the system.
22. Amari S. Biol Cybern 1977;27:77. [PubMed: 911931]
23. Marder M, Gross S. J Mech Phys Solids 1995;43:1.
24. Telfeian AE, Connors BW. Epilepsia 1998;39:700. [PubMed: 9670897]
25. Connors BW. Nature (London) 1984;310:685. [PubMed: 6147755]
26. Chervin RD, Pierce PA, Connors BW. J Neurophysiol 1988;60:1695. [PubMed: 3143812]

Acknowledgements

This work was supported by the Whitaker Foundation Grant No. RG990432 and NIH Grants No. K02MH01493 and No. R01MH50006. We are grateful to D. J. Pinto, G. B. Ermentrout, and E. Sander for helpful discussions.

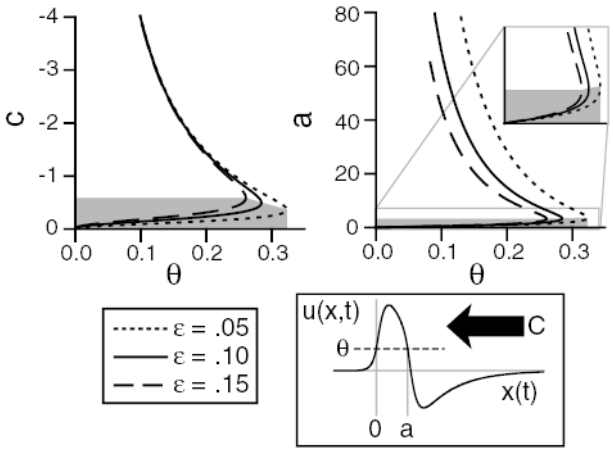

FIG. 1.

Relationships between model parameters. For a given threshold (θ) and relative time constant (ϵ) there are either 2 or 0 solutions of speed (*c*) and width (*a*). The solutions in the gray regions are unstable. An example of a stable traveling pulse solution is shown in the inset (ϵ = 0.10, θ= 0.25).

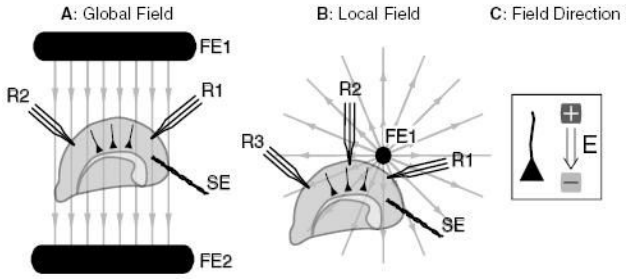

FIG. 2.

Schematic of global field (a) and local field (b) experiments. (a) Large Ag/AgCl electrodes (FE1, FE2) embedded in the interface chamber floor were used to apply the global electric field. (b) A small Ag/AgCl cylindrical pellet (FE1) placed close to the pial surface was used to apply a local electric field, and a reference electrode was placed in the artificial cerebrospinal fluid far from the slice. (c) Direction of a positive field from FE1 relative to dendrite-soma axis of pyramidal cells in layer 5 (triangle denotes soma).

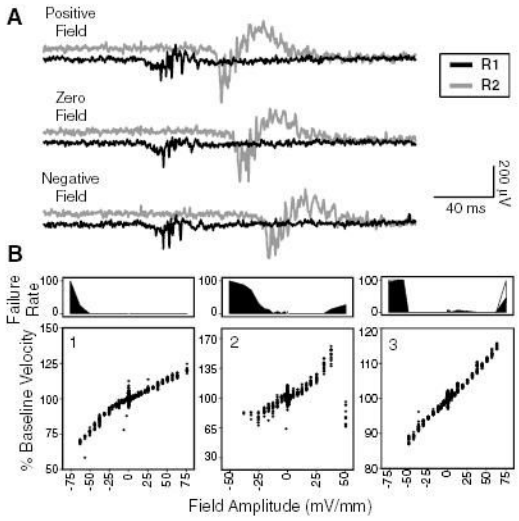

FIG. 3.

Global field results. (a) Extracellular recordings are made during positive (top traces), zero (middle traces), and negative (lower traces) electric field application. The activity wave arrived at R2 earlier during positive field (top) and later during negative field (lower) relative to zero field (middle) application. (b) Wave speed (bottom) normalized by baseline speed and failure rate (top) as a function of field amplitude is shown for three separate experiments. As the field amplitude became more positive (negative), the speed increased (decreased). As the field amplitude became increasingly negative, propagation failure rate increased to complete failure.

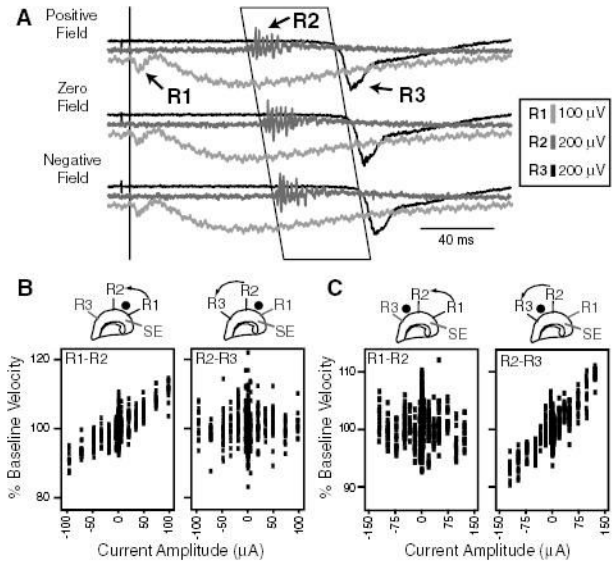

FIG. 4.

Local field results. (a) Extracellular recordings made during the positive (top traces), zero (middle traces), and negative (bottom) local field application is shown. Waveforms associated with each electrode (R1, R2, or R3) are labeled accordingly. The activity travel time between R2 (left edge of the parallelogram) and R1 (black vertical line) varied with applied field amplitude. Alternatively, travel time is independent of the applied field amplitude between R2 (left edge of parallelogram) and R3 (right edge of parallelogram) where the electric field is smaller and not aligned with the neurons. (b),(c) Wave speed normalized by baseline velocity as a function of field amplitude for two experiments is shown. In (b), the field was applied (locally aligned with the neurons) between R1 and R2. In (c), the field was applied between R2 and R3. In either case, within the applied field, speed increased (decreased) with increasingly positive (negative) field amplitude, and was independent of amplitude outside the electric field.